



## Rational discovery of a highly novel and selective mTOR inhibitor

Stanley Jin<sup>a,b,\*</sup>, Satoshi Mikami<sup>a,1</sup>, Nick Scolah<sup>a</sup>, Young Chen<sup>a,2</sup>, Petro Halkowycz<sup>a</sup>, Lihong Shi<sup>a,2</sup>, Jason Kahana<sup>a,3</sup>, Patrick Vincent<sup>a</sup>, Ron de Jong<sup>a</sup>, Joy Atienza<sup>a</sup>, Robyn Fabrey<sup>a</sup>, Lilly Zhang<sup>a,4</sup>, Matthew Lardy<sup>a,5</sup>

<sup>a</sup> Takeda California, 10410 Science Center Drive, San Diego, CA 92121, United States

<sup>b</sup> Fronthera US Pharmaceuticals, LLC, San Diego, CA, USA

### ARTICLE INFO

**Keywords:**  
mTOR  
SBDD  
Inhibitor

### ABSTRACT

Aided by Structure Based Drug Discovery (SBDD), we rapidly designed a highly novel and selective series of mTOR inhibitors. This chemotype conveys exquisite kinase selectivity, excellent in vitro and in vivo potencies and ADME safety profiles. These compounds could serve as good tools to explore the potential of TORC inhibition in various human diseases.

The mammalian target of rapamycin (mTOR), is a member of the phosphatidylinositol 3-kinase-related kinase family of protein kinases,<sup>1</sup> which includes two distinct complexes: mTOR complex 1 (mTORC1) and mTOR complex 2 (mTORC2). As a serine/threonine protein kinase, mTOR regulates protein synthesis, cell growth and proliferation. In addition, mTOR has been shown to regulate the ability of tumors to promote angiogenesis as well as the response of tumor cells to nutrients and growth factors. Thus, inhibitors of mTOR are considered as a target for immunosuppression, leukemia, and cancer treatment et al.<sup>2–5</sup>

As the first potent, synthetic mTOR inhibitor, **PI-103** is a multi-targeted PI3K inhibitor for p110 $\alpha$ / $\beta$ / $\delta$ / $\gamma$ .<sup>6</sup> It potently inhibits both the rapamycin-sensitive (mTORC1) and rapamycin-insensitive (mTORC2) complexes of the protein kinase mTOR.<sup>7</sup> Also, **PI-103** is a potent ATP-competitive dual inhibitor of phosphatidylinositol 3-kinase (PI3K) and mTOR.<sup>8</sup> By inhibiting mTOR activity, **PI-103** induces autophagy and promotes cell apoptosis.<sup>9,10</sup> In order to improve the properties of this lead, structural modification of **PI-103** led to the discovery of **Compound 1** (Fig. 1), a quaternary-substituted dihydrofuranpyrimidine, which was found to inhibit human mTOR with a pIC<sub>50</sub> of greater than 7.5.<sup>2,11</sup> It was suggested that this quaternary structure would provide additional selectivity over the PI3K, while blocking a benzylic position was expected to reduce metabolism.<sup>12</sup>

By studying the structure–activity relationship (SAR) of mTOR inhibitors in the literature,<sup>2,13–15</sup> we found that the general mTOR

binding mode consists of a pyrimidine core incorporating a morpholine hinge-region binding group, and a back pocket. Most of those fragments have been well studied and optimized in the past decades, and numerous potent mTOR inhibitors were reported. Based on the SAR of this series that morpholine moiety plays an important role in the mTOR potency,<sup>14</sup> we found that no related efforts have been reported to focus on the conformation study between the morpholine moiety and the pyrimidine core. This consideration brought us to hypothesize that this circled region would be worth studying (Fig. 2). The conformation of the previous mTOR inhibitors was uncertain due to its binding pattern between the pyrimidine and the morpholine. Thus, we hypothesized that the introduction of the ring fusion would keep the coplanarity and fix the conformation of the morpholine moiety and pyrimidine core, which would also occupy the corresponding region.

Molecular modeling by structure-based drug design (SBDD) techniques suggested that the six-member ring-fused molecule best fits in the pocket, comparing to the five- and seven-member fused-ring molecules. Thus, we designed and synthesized four targets (**Compound 2**, **Compound 3**, **Compound 4** and **Compound 5**, as shown in Fig. 3), and ran the assay for the mTOR/PI3K inhibition to validate the molecular modeling result. Consistent with modeling analyses, we observed that analogues with six-member fused rings showed better mTOR inhibition (pIC<sub>50</sub> > 6) than five- and seven-member rings (pIC<sub>50</sub> < 6). However, the selectivity of mTOR inhibition over PI3K $\alpha$  was low (e.g. pIC<sub>50</sub> = 6.5

\* Corresponding author at: 11526 Sorrento Valley Road, STE D, San Diego, CA 92121, United States.

E-mail addresses: [stanjin@frontherapharma.com](mailto:stanjin@frontherapharma.com) (S. Jin), [patrick.vincent313@att.net](mailto:patrick.vincent313@att.net) (P. Vincent), [mlardy@predictivenumerics.com](mailto:mlardy@predictivenumerics.com) (M. Lardy).

<sup>1</sup> Takeda Pharmaceutical Company Limited, Kanagawa, Japan.

<sup>2</sup> Celgene, 10300 Campus Point Drive, Ste 100, San Diego, CA 92121, United States.

<sup>3</sup> Integrity Biosolutions, 8724 Butano Ct, San Diego, CA 92129, United States.

<sup>4</sup> Simcere Pharmaceutical Group.

<sup>5</sup> Predictive Numerics.

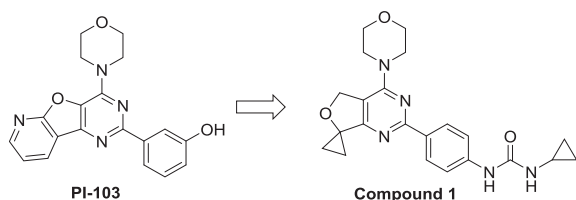


Fig. 1. Structural modification of PI-103 led to the discovery of Compound 1.

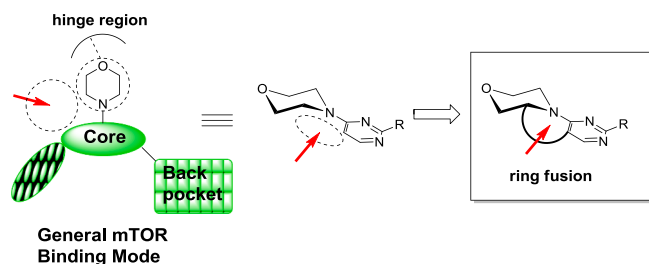


Fig. 2. SAR study of mTOR inhibitors.

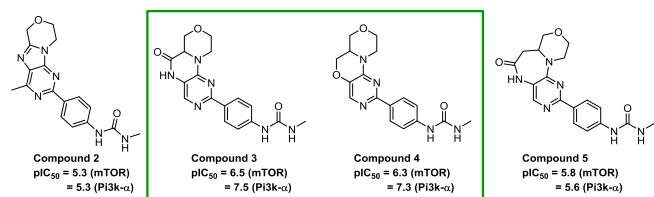
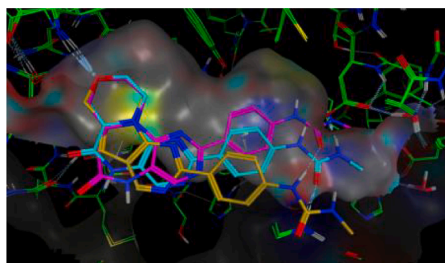


Fig. 3. SBDD-aided molecular modeling and mTOR/PI3K $\alpha$  inhibition results of the designed targets.

for mTOR/7.5 for PI3K $\alpha$ , Fig. 3).

In order to improve the selectivity of mTOR inhibition over PI3K $\alpha$ , further optimization of Compound 3 was carried out (Fig. 4). The mTOR inhibition (pIC<sub>50</sub> = 7.5) was increased by *N*-alkylation of the fused amide. The corresponding PI3K $\alpha$  inhibition (pIC<sub>50</sub> = 7.7) was not

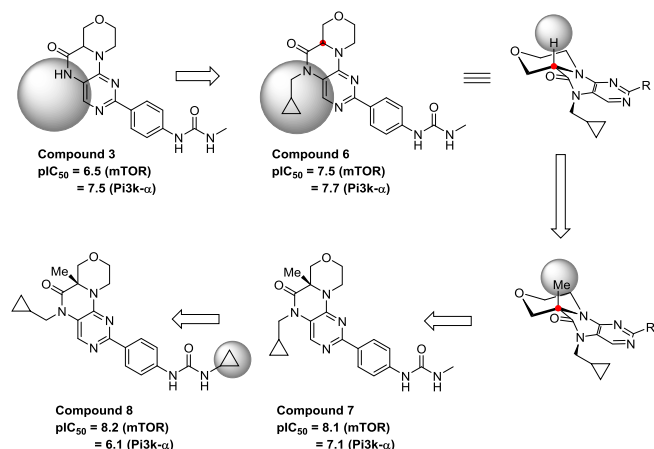
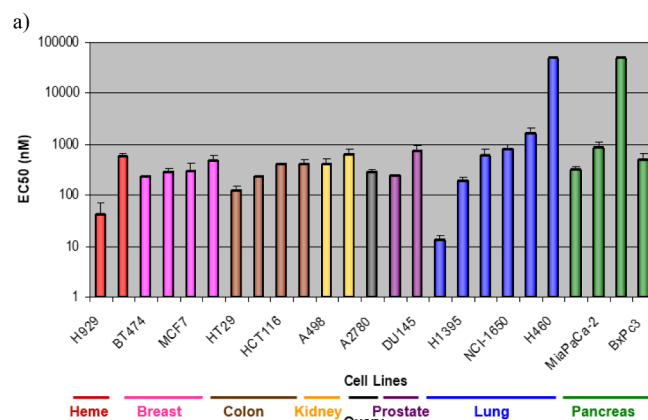


Fig. 4. The discovery process of Compound 8.

improved much, and the selectivity of mTOR inhibition over PI3K $\alpha$  was still not ideal. It was reported that the replacement of morpholine by a substituted morpholine with certain chirality significantly improved mTOR potency and selectivity over PI3K $\alpha$ .<sup>14</sup> Thus, by studying the stereochemistry of Compound 6, we found that the replacement of the proton at the axial position with methyl group might reach our expectation. By synthesizing the target compound Compound 7 with desired chirality, we observed that the mTOR inhibition was further increased (pIC<sub>50</sub> from 7.5 to 8.1), while its corresponding PI3K $\alpha$  inhibition was decreased (pIC<sub>50</sub> from 7.7 to 7.1). Further optimization on the substitution group on the urea from methyl to cyclopropyl gave much better mTOR inhibition selectivity over PI3K $\alpha$ . Thus, the mTOR inhibition selectivity over PI3K $\alpha$  was increased by 1000-fold during the whole optimization from Compound 3 to Compound 8 within 2 months. Synthetically, the methyl group could only be at the axial position. Further optimization showed that Compound 9 exhibited both slightly better mTOR inhibition activity and selectivity over PI3K $\alpha$  than Compound 8.<sup>16</sup>

One lead compound, Compound 9 (mTOR pIC<sub>50</sub> = 7.9; PI3K $\alpha$  pIC<sub>50</sub> = 5.9) showed broad potencies in a variety of cancer cell lines (Fig. 5a). Generally, cancer cell lines of blood, breast, colon, kidney and ovary origins showed relatively increased sensitivity to TORC inhibition by Compound 9. Combined treatments of Compound 9 with EGFRi (erlotinib) or gemcitabine caused synergistic effects in LKB1/KRASmut NSCLC cell lines (Fig. 5b). No correlation between combination effect and EGFR status was observed. Additive effects were observed when Compound 9 was combined with PI3K $\alpha$  inhibitor GDC-0941, Rafi (sorafenib), and BCL2i (ABT-737).

Compound 9 also proved highly potent in a number of xenograft efficacy studies. For example, partial regressions were observed in a



b)

Cell line	Rx	Erlotinib (EGFR <sub>i</sub> )	Gemcitabine (DNA synthesis <sub>i</sub> )
A549 LKB1mut, KRAS (G12S)		Syn	Syn
H460 LKB1mut, KRAS (G61H)		Syn	Syn
H1395 LKB1mut, BRAF (G469A)		Add	Add
H1650 EGFR (E746_A750del)		Add	Add
H1975 EGFR (L585R, T790M)		Add	Add
H292 WT		Add	Add

Fig. 5. a) Shows potent in vitro activity of Compound 9 against a broad range of cancer cell lines; b) Effect of Erlotinib and Gemcitabine with LKB/KRASmut cell lines. Effects above additive were considered synergistic.

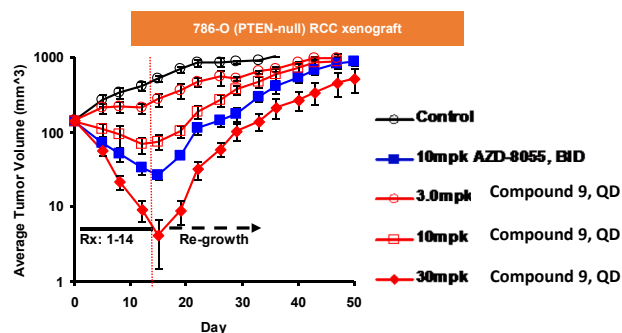
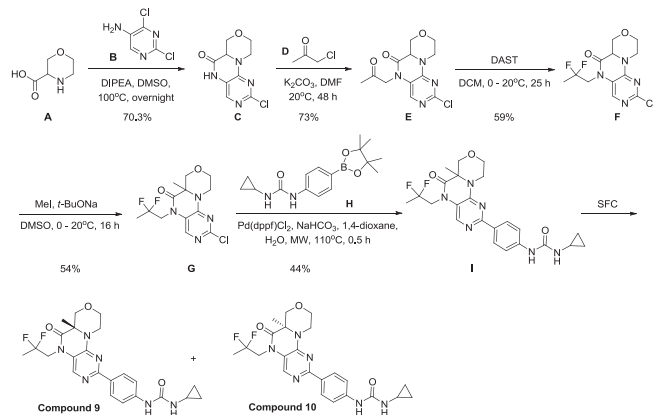


Fig. 6. Compound 9 exhibits excellent tumor growth inhibition.



Scheme 1. Synthesis of Compound 9.

786-O xenograft study at 30 mpk QD, (Fig. 6). Treatment was well tolerated while maintaining a < 10% body weight.

The preparation of target compound **Compound 9** was described in Scheme 1. The target compound was synthesized from commercially available 3-morpholinecarboxylic acid **A** via 6 steps. The initial cyclization of piperazinone ring was resulted from 3-morpholinecarboxylic acid **A** and 5-amino-2,4-dichloropyrimidine **B** in 70.3% yield. *N*-alkylation of compound **C** using chloroacetone afforded compound **E** in 73% yield, which was subsequently fluorinated by DAST under mild condition to give di-fluoro intermediate **F** in 59% yield. After treating **F** with strong base, the *C*-alkylation was realized by addition of methyl iodide in 54% yield. Suzuki coupling reaction between **G** and *para*-urea substituted phenylboronic ester **H** afforded the racemic target compound **I** in 44% yield. Final chiral separation afforded the desired target **Compound 9**.

In summary, we first carefully studied the SAR of both literature and in-house mTOR and PI3K $\alpha$  inhibitors to gain knowledge on the subtle differences of the mTOR and PI3K $\alpha$  binding pockets. This knowledge in turn inspired us to come up with design hypotheses, which we methodically interrogated and prioritized with the aid of SBDD. The initial hit **Compound 3** was actually 10-fold PI3K $\alpha$  selective. However, a clear understanding of the chemotype's conformation resulted in the breakthrough design element of a pseudo-axial methyl group, which ultimately gave us excellent (> 100-fold) mTOR selectivity over PI3K $\alpha$ . This chemotype conveys exquisite kinase selectivity, excellent in-vitro and in-vivo activity along with desired ADME safety profiles. These compounds could serve as good tools to explore the potential of TORC inhibition in various human diseases.

In vitro and in vivo assays were performed as outlined in: Farrell PJ, Matuszkiewicz J, Balakrishna D, Pandya S, Hixon MS, Kamran R, Chu S, Lawson JD, Okada K, Hori A, Mizutani A, Iwata H, de Jong R, Hibner B,

Vincent P. MET tyrosine kinase inhibition enhances the antitumor efficacy of an HGF antibody. *Mol Cancer Ther.* 2017 Jul; 16(7):1269–1278.

#### mTor assay

#### Materials

FRAP1(mTor) recombinant protein and GFP-4E-BP1 were purchased from Invitrogen. (Carlsbad, CA, US) The kinase activity assay was conducted in 50 mM Hepes buffer containing 10 mM MgCl<sub>2</sub>, 0.01% Brij, 0.2 mM EDTA, 2 mM DTT and 1% DMSO (after compound addition) at pH 7.3.

#### Methods

**IC<sub>50</sub> determination** – the IC<sub>50</sub> value for each compound was determined in the presence of compound (various concentrations, from 0 to 10  $\mu$ M) and a fixed amount of ATP (50  $\mu$ M, final concentration), substrate GFP-4E-BP1 (400 nM, final concentration). The enzymatic reaction was initiated by adding FRAP1(mTor) (2 nM, final concentration). The assay was conducted at room temperature (~22 °C). After 30 min, the enzymatic reaction was stopped using Tb-anti-p4E-BP1 (2 nM final concentration, Invitrogen) and EDTA (20 mM final concentration, Sigma) in TR-FRET dilution buffer provided by Invitrogen. All the reagents were dispensed using a Multidrop Combi reagent dispenser (ThermoFisher Scientific, Waltham, MA US) into black 384 SV Greiner plates. The release of product was detected using a BMG PHERAstar plate reader (BMG LABTECH, Ortenberg, Germany) and the Lantha Screen module (337 nm (excitation wavelength) and measuring the ratio of fluorescence 520/490 nm (emission wavelengths). Experimental data was fitted using Eq. (1):

$$\frac{V_i}{V_o} = \frac{100}{1 + \left(\frac{I}{IC_{50}}\right)^n}$$

$V_i$  and  $V_o$  are the rates of the enzyme activity in the presence and in the absence of inhibitor;  $n$  is the Hill coefficient;  $I$  is the free inhibitor concentration, respectively;  $IC_{50}$  is a measure of potency that is equivalent to a concentration of inhibitor that leads to a 50% inhibition of the enzyme activity.

#### Appendix A. Supplementary data

Supplementary data to this article can be found online at <https://doi.org/10.1016/j.bmcl.2019.126659>.

#### References

- [1]. Mitra A, Luna JI, Marusina AI, et al. *J Invest Dermatol.* 2015;135:2873.
- [2]. Dong, Q.; Jin, B.; Lardy, M.; Zhao, F. U.S. Pat. Appl. 2011021515, 2011.
- [3]. Giles FJ, Albitar M. *Curr Mol Med.* 2005;5:653.
- [4]. Zhang L, Bu T, Bao X, et al. *Bioorg Med Chem Lett.* 2017;27:3395.
- [5]. Faivre S, Kroemer G, Raymond E. *Nat Rev Drug Discovery.* 2006;5:671.
- [6]. Hayakawa M, Kaizawa H, Moritomo H, et al. *Bioorg Med Chem Lett.* 2007;17:2438.
- [7]. Knight ZA, Gonzalez B, Feldman M, et al. *Cell.* 2006;125:733.
- [8]. Schenone S, Brullo C, Musumeci F, Radi M, Botta M. *Curr Med Chem.* 2011;18:2995.
- [9]. Fan Q, Weiss WA. *Autophagy.* 2011;7:536.
- [10]. Park S, Chapuis N, Bardet V, et al. *Leukemia.* 2008;22:1698.
- [11]. Jin, B.; Lardy, M.; Zhou, F.; Dong, Q. WO 2012099581 A1, 2012.
- [12]. Cohen F, Bergeron P, Blackwood E, et al. *J Med Chem.* 2011;54:3426.
- [13]. Sutherland DP, Sampath D, Berry M, et al. *J Med Chem.* 2010;53:1086.
- [14]. Verheijen JC, Yu K, Toral-Barza L, Hollander I, Zask A. *Bioorg Med Chem Lett.* 2010;20:375.
- [15]. Kaplan J, Verheijen JC, Brooijmans N, et al. *Bioorg Med Chem Lett.* 2010;20:640.
- [16]. Jin, B.; Scora, N.; Dong, Q. U.S. Pat. Appl. 20110053921, 2011.